Electronic Supplementary information

Ultrahigh water permeance of reduced graphene oxide nanofiltration membrane for multivalent metal ions rejection

Fangfang Dai,[a,†] Risheng Yu,[a,†] Ruobing Yi,[a] Jian Lan,[b] Rujie Yang, [a] Zhikun Wang,[a]

Junlang Chen,[a,*] Liang Chen,[a,*]

[a.] *Department of Optical Engineering, Zhejiang Prov Key Lab Carbon Cycling Forest Ecosy, College of Environmental and Resource Sciences, Zhejiang Provincial Key Laboratory of Chemical Utilization of Forestry Biomass, Zhejiang A&F University, Hangzhou 311300, China*

[b.] *College of Pharmaceutical Chemistry and Materials Engineering, Taizhou University, Taizhou, Zhejiang 317000, China*

† These authors contributed equally to this work: Fangfang Dai, Risheng Yu

*Corresponding author. E-mail: liangchen@zafu.edu.cn (L.C.); chenjunlang7955@sina.com (J.C.)

Contents

PS1 Materials and methods

Preparation of rGO suspension

The small size GO was prepared using an improved Hummer's method using the method described in previous work [S1-S3]. 30 mL of 3.5 mg/mL GO suspension was mixed with 360 mL 28% NH_4OH and 570 mL DI water. Then the mixed solution was stirred at 80℃ for 6 hours and further stirred at 90℃ for 1 hour. Finally, the concentration of the prepared AH-rGO suspension was approximately 17 μg/mL.

AH-rGO membrane fabrication

AH-rGO membranes supported by the mixed of cellulose ester (MCE; 0.22 μm pores) was fabricated by vacuum filtration method. The AH-rGO membranes with different thicknesses were prepared from 40mL of 8.5 mg/L, 21.3 mg/L, 42.5 mg/L, 63.8 mg/L, 85.0 mg/L of AH-rGO suspension under a pressure of 1 bar, with corresponding thicknesses from 160 nm to 1600 nm which were denoted as AH-rGO-160, AH-rGO-400, AH-rGO-800, AH-rGO-1200 and AH-rGO-1600, respectively. These AH-rGO membranes were used as nanofiltration membranes in this work.

PS2 Characterization methods

The morphology of AH-rGO membranes was observed by a field-emission scanning electron microscope (SEM, SU 8000 series) operated at an accelerating voltage of 5 kV. The XPS measurement was carried out on hermo Fisher ESCALAB 250Xi spectrometer. Salt concentrations were measured using inductive coupled plasma-optical emission spectrometry (ICP-OES).

The C1s spectra was divided into five Gaussian peaks at 284.5, 286.4, 287.7, 288.88 and 285.8 eV, which correspond to the typical signals of C-C/C=C, C-OH, C-O-C, O=C-OH and C-N, respectively[S3-S6].

PS3 Experimental setup for rejection experiment

After the preparation of the AH-rGO membrane, six salt solutions of $FeCl_3$, $AlCl_3$, $CrCl_3$, $CuSO_4$, $ZnSO_4$ and $Pb(NO_3)_2$ were added to the feed side of the dead-end filtration set up. Under a pressure of 1 bar, the salt solutions were filtered through AH-rGO membranes. Filtrates were collected after 20 min when the filtration process became steady. The water permeance (J_w) and Rejection rate (R) were respectively calculated by using the following equation:

$$J_w = \frac{V}{\Delta t \times A \times P}$$

$$R = (1 - \frac{C_P}{C_f}) \times 100\%$$

where J_W is the water permeance (L m^{-2} h^{-1} bar^{-1}), V is the volume of the filter liquor (L), A is the effective membrane area (m^2). Δt is the permeance time (h), and the P is the filtration pressure (bar). C_p and C_f are the concentrations of permeate and feed ions solutions, respectively, which were measured by inductive coupled plasma-optical emission spectrometry (ICP-OES).

PS4 Experimental setup for long-term experiment of AH-rGO membranes

The water permeance and rejection rate of the AH-rGO-800 membranes for long-term experiment were analyzed for 7 days. 2000 mL of 50 mg/L $Pb(NO_3)_2$ solution is prepared in a beaker, and then delivered the solution to the feed side with a peristaltic pump, maintained ~100mL solution in the feed side, formed a cyclic flow between the feed side and the beaker. We recycled the filtrates into the beaker to maintain a stable salt concentration in the feed. After running for 24 hours under vacuum filtration,

collecting filtrates to measure the rejection and water flux.

Table S1. Long-term performance measurements of the AH-rGO-800 membranes for the 50 mg/L $Pb(NO_3)_2$ solution for 7 days.

Days	Feed size (mg/L)	Error (mg/L)	Filtrates (mg/L)	Error (mg/L)	Rejection rate%	Permeance (L m^{-2} h^{-1} bar^{-1})
1	46.4	0.3	3.0	0.1	93.5	43.6
2	43.7	0.6	3.5	0.3	92.1	44.8
3	45.0	1.0	3.5	0.5	92.1	40.2
4	49.1	0.1	3.1	0.1	93.7	36.0
5	45.2	0.1	3.0	0.1	93.5	33.4
6	49.1	3.7	3.1	0.1	93.7	33.7
7	48.9	3.5	4.5	2.4	90.7	33.0

PS5 Filtration performance of the nanofiltration membranes reported in literature in terms of water permeance and rejection rates for multivalent ions.

Table S1 Comparisons of different nanofiltration membranes in water permeance and rejection rates for multivalent metal ions in literature.

Membrane	Application	Water flux (L m^{-2} h^{-1} bar^{-1})	Rejection (%)	Ref.
Nematic multi layered GOMs	Monovalent and divalent ions	71	30~40	S7
MWCNT intercalated	Na_2SO_4, NaCl, $MgSO_4$, $MgCl_2$	11.3	9.5~95.1	S8
rGO membrane HNTs anchored on the commercial NF membrane	Cu^{2+}	13.9	74.3	S9

POSS nanoparticles and MMA on the PEI membranes	Na_2SO_4, $CrSO_4$, $Pb(NO_3)_2$ and $Cu(NO_3)_2$	14.3	79~84	S10
GO/Torlon hollow fiber membrane	Pd^{2+}, Ni^{2+}, Zn^{2+}	4.7	95.9~98.1	S11
GO-IPDI membrane	Cu^{2+}, Pb^{2+}, Cr^{3+}, Cd^{2+}	55-90	47~57 （Cu^{2+}）	S12
PSE-GO-DMF	Cu^{2+}, Pb^{2+}, Cr^{3+}, Cd^{2+}	~100	90	S13
LBL-GO/PEI	Na^+, Mg^{2+}	4.2	Na:38 Mg:93	S14
γ-Al_2O_3 NF membrane	Fe^{3+}, Al^{3+}, Mg^{2+}, Ca^{2+}, Na^+, NH_4^+	17.4	27.3~97.1	S15
rGOM	**$FeCl_3$, $AlCl_3$, $CrCl_3$, $CuSO_4$, $ZnSO_4$, $Pb(NO_3)_2$**	**31.2~142.5**	**91.6-99.9**	**This study**

PS6 Ions adsorption of the AH-rGO membranes.

We analysed the ions adsorption of AH-rGO membranes during the filtration process. Our previous studies on adsorption of $Pb(NO_3)_2$ by rGO membranes have demonstrated that the ions adsorption mainly occurred within the first 20 min, and then reached adsorption equilibrium with a corresponding adsorption capacity of 0.17 g/g[31]. Therefore, the filtrates were collected after 20 min when the filtration process became steady in this work. The total filtrates have exceeded 30 mL including 15~20 mL in the first 20 min together with ~15 mL collected later. So that the total salts removed in the filtrates were about 1.5~7.5 mg (at least 30 mL of 50~250 mg/L $Pb(NO_3)_2$ solutions). Besides, the AH-rGO-800 membrane used in a filtration experiment was about 1.7 mg (prepared from 40 mL of 42.5 mg/L AH-rGO suspensions). Thus, the adsorption capacities reached 0.88~4.41 g/g, if we assumed that the ions removal of the filtrates could be totally explained by adsorption. Such assumed adsorption capacity derived

from the ~30 mL filtrates (not the total salt solution of 100 mL), are much higher than the adsorption capacity of 0.17 g/g in our previous work. Moreover, our AH-rGO-800 membranes have outstanding stability over long-term operation, which will results in incredible adsorption capacities based on the assumption. Therefore, the significant effect on removal multivalent ions here is mainly due to the rejection by AH-rGO membranes, even though the adsorption effect could not be negligible. For the high salts concentration or the permeation of long-term operation, the salts removal were almost entirely due to the rejection rather than adsorption by AH-rGO membranes.

PS7 Water performance and rejection rates of AH-rGO membranes for $MgSO_4$ and Na_2SO_4.

We have further new performance tests for 50 mg/L $MgSO_4$ and Na_2SO_4 solutions, as shown in Fig. S1. The water permeance for AH-rGO membranes were 38.0 and 48.6 L m^{-2} h^{-1} bar^{-1} with corresponding rejection rates of 91.4% and 45.4% for $MgSO_4$ and Na_2SO_4 solutions, respectively. The result shows a moderate performance of AH-rGO membranes for $MgSO_4$ and Na_2SO_4 solutions.

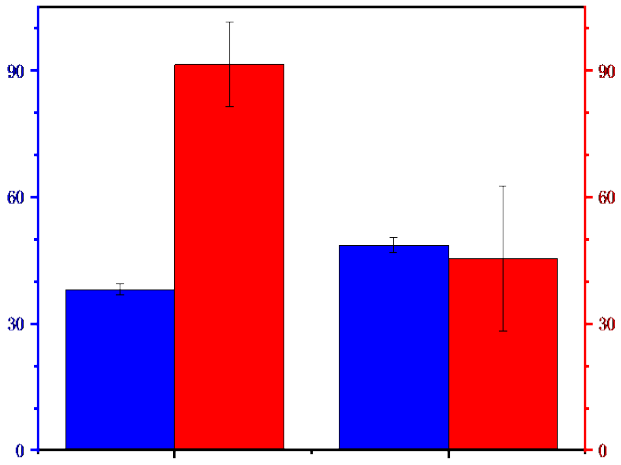

Fig. S1. Water performance and rejection rates of AH-rGO membranes for 50 mg/L $MgSO_4$ and Na_2SO_4 solutions.

References

S1. H. Yi, X. Zhen and G. Chao, *Advanced Functional Materials*, 2013, **23**, 3693-3700.

S2. E. C. Garnett and P. Yang, *Journal of the American Chemical Society*, 2008, **130**, 9224-9225.

S3. L. Zhang, F. Dai, R. Yi, Z. He, Z. Wang, J. Chen, W. Liu, J. Xu and L. Chen, *Applied Surface Science*, 2020, **520**, 146308.

S4. C.-H. Lee, J.-M. Yun, S. Lee, S. M. Jo, S. J. Yoo, E. A. Cho, M.-S. Khil and H.-I. Joh, *Materials Research Bulletin*, 2014, **59**, 145-149.

S5. R. Lv, Q. Li, A. R. Botello-Mendez, T. Hayashi, B. Wang, A. Berkdemir, Q. Hao, A. L. Elias, R. Cruz-Silva, H. R. Gutierrez, Y. A. Kim, H. Muramatsu, J. Zhu, M. Endo, H. Terrones, J. C. Charlier, M. Pan and M. Terrones, *Sci Rep*, 2012, **2**, 586.

S6. X. Yang, K. Li, D. Cheng, W.-L. Pang, J. Lv, X. Chen, H.-Y. Zang, X.-L. Wu, H.-Q. Tan, Y.-H. Wang and Y.-G. Li, *Journal of Materials Chemistry A*, 2018, **6**, 7762-7769.

S7. A. Akbari, P. Sheath, S. T. Martin, D. B. Shinde, M. Shaibani, P. C. Banerjee, R. Tkacz, D. Bhattacharyya and M. Majumder, *Nature Communications*, 2016, **7**, 10891.

S8. Y. Han, Y. Jiang and C. Gao, *Acs Applied Materials & Interfaces*, 2015, **7**, 8147.

S9. X. Liu, P. Feng, L. Zhang and Y. Chen, *Polymers for Advanced Technologies*, 2020, **31**, 997-1006.

S10. N. Haninah, Z. Z. Abidin, A. H. Abdullah and R. Othaman, *Processes*, 2020, **8**, 230.

S11. Q. Nan, P. Li and B. Cao, *Applied Surface Science*, 2016, **387**, 521-528.

S12. P. Zhang, J. L. Gong, G. M. Zeng, C. H. Deng, H. C. Yang, H. Y. Liu and S. Y. Huan, *Chemical Engineering Journal*, 2017, **322**, 657-666.

S13. R. Mukherjee, P. Bhunia and S. De, *Chemical Engineering Journal*, 2016, 284-297.

S14. Q. Nan, P. Li and B. Cao, *Applied Surface Science*, 2016, **387**, 521-528.

S15. Z. Wang, Y.-M. Wei, Z.-L. Xu, Y. Cao, Z.-Q. Dong and X.-L. Shi, *Journal of Membrane Science*, 2016, **503**, 69-80.